Helicity of Electrons from μ^- Decay*†

DANIEL M. SCHWARTZ‡
Department of Physics and The Enrico Fermi Institute for Nuclear Studies, The University of Chicago, Chicago, Illinois

(Received 12 April 1967)

The helicity of electrons from μ^- decay has been measured using the spin dependence of electron-electron (Møller) scattering. A magnetized foil (Supermendur) was used as a target of polarized electrons. Optical spark chambers, scintillators, and decision-making spark chambers were used to detect the scattering events, and the pictures were measured with an automatic film scanning system (CHLOE). The experimental method and the data processing system reduced the systematic error due to background events below that of previous experiments. The helicity was found to be -0.89 ± 0.28.

I. INTRODUCTION

THE helicity of electrons and positrons from muon decay has been measured by several authors[1,2] and has generally been found to be consistent with the predictions of the $V-A$ theory. However, because of the difficulty of the experiment, the errors caused by statistical and systematic uncertainties in the background rates and by other systematic effects are rather large. Previous experiments on μ^- decay electrons[1] do not quote a value for the helicity, but state that their results are consistent with -1. The measurements of the helicity of positrons from μ^+ decay,[2] with the possible exception of that of Dick *et al.*,[3] are all consistent with $+1$. The most recent of these experiments (Duclos *et al*). gives the result $+1.04\pm0.18$ for positrons.

Jarlskog[4] has shown that the strongest restriction which can be placed on the form of the muon decay interaction from determinations of the observable parameters comes from a measurement of the helicity, $h=\langle\hat{\sigma}\cdot\hat{p}\rangle$.

She shows that if one defines the coupling constants g_i and g_i' by using

$$\mathcal{H}=\sum[\bar{\psi}_e(g_i+g_i'\gamma_5)O_i\psi_\mu](\bar{\psi}_{\nu_\mu}O_i\psi_{\bar{\nu}_e})+\text{H.c.} \quad (1)$$

as the interaction Hamiltonian ($i=S, V, T, A, P$), then the condition $h=-1$ for μ^- decay results in $g_i'=-g_i$ (all i) thus reducing the number of unknown complex constants from ten to five. [Note that Eq. (1) differs from the usual convention in that here the $(g_i+g_i'\gamma_5)$ factor is put in the bracket containing the charged-particle wave functions. The motivation for this formulation comes from the fact that the neutrinos are not observed in the usual muon decay experiments.]

Jarlskog further shows that the nominal $V-A$ values for the parameters suffice only to confine the interaction to V and A; and without the assumption of two-component neutrinos, one can say nothing about g_A/g_V.[5] Specifically, the values $\rho=\frac{3}{4}$, $\xi=1$, and $\delta=\frac{3}{4}$, along with unit helicity of the decay electrons, are shown to imply $g_i'=g_i=0$ for $i=S, T, P$, $g_V'=-g_V$, and $g_A'=-g_A$. These restrictions lead to an interaction Hamiltonian of the form[6]

$$\mathcal{H}=g_V\Big[(\bar{\psi}_e\gamma_\mu(1+\gamma_5)\psi_\mu)\times\Big(\bar{\psi}_{\nu_\mu}\gamma_\mu\Big(1-\frac{g_A}{g_V}\gamma_5\Big)\psi_{\bar{\nu}_e}\Big)\Big]+\text{H.c.} \quad (2a)$$

In the current-current formalism, the Hamiltonian can be written

$$\mathcal{H}=S(\bar{\psi}_e(1-\gamma_5)\psi_{\bar{\nu}_e})(\bar{\psi}_{\nu_\mu}(1+\gamma_5)\psi_\mu)+V(\bar{\psi}_e\gamma_\mu(1+\gamma_5)\psi_{\bar{\nu}_e})(\bar{\psi}_{\nu_\mu}\gamma_\mu(1+\gamma_5)\psi_\mu)+\text{H.c.} \quad (2b)$$

where $S=-(g_V+g_A)$ and $V=\frac{1}{2}(g_V-g_A)$.

Jarlskog also notes that the experimental uncertainty in the value of the helicity plays the dominant role in an attempt to place upper limits on the S, T, and P contributions. She shows that the available experimental information about the muon decay parameters, including current values for experimental errors, does not rule out the possibility of large admixtures of tensor,

* Research supported by the U. S. Office of Naval Research.

† A thesis submitted to the Department of Physics, The University of Chicago, in partial fulfillment of the requirements for the Ph.D. Degree.

‡ Present address: Physics Department, The Ohio State University, Columbus, Ohio.

[1] P. C. Macq, K. M. Crowe, and R. P. Haddock, Phys. Rev. **112**, 2061 (1958); G. Culligan, S. G. F. Frank, and J. R. Holt, Proc. Phys. Soc. (London) **73**, 169 (1959).

[2] L. Dick, L. Feuvrais, and M. Spighel, Phys. Letters **7**, 150 (1963); A. Buhler, N. Cabibbo, M. Fidecaro, T. Massam, Th. Muller, M. Schneegans, and A. Zichichi, *ibid.* **7**, 368 (1963); S. Bloom, L. A. Dick, L. Feuvrais, G. R. Henry, P. C. Macq, and M. Spighel, Phys. *ibid.* **8**, 87 (1964); J. Duclos, J. Heintze, A.De Rujula, and V. Soergel, *ibid.* **9**, 62 (1964).

[3] The helicity result for positrons ($+0.28\pm0.16$) given by Dick *et al.* (Ref. 2) should be interpreted in the light of subsequent experiments on the depolarization of positrons in Be moderator. [See L. Dick, L. Feuvrais, L. Di Lella, and M. Spighel, Phys. Letters **10**, 236 (1964); W. Chinowsky, D. Cutts, and R. Steining, Nuovo Cimento **34**, 1431 (1964).] These experiments indicate the existence of an unexplained depolarization mechanism which could account for the helicity result of Dick *et al.*

[4] C. Jarlskog, Nucl. Phys. (Neth.) **75**, 659 (1966).

[5] Furthermore, the low-energy spectrum parameter η becomes equal to zero when the result $g_i'=-g_i$ is applied. Therefore, if the helicity of the decay $e^\pm$ is ±1.0, no additional information is gained by measuring η.

[6] For a discussion, see V. L. Telegdi, in Proceedings of the Argonne International Conference on Weak Interactions, 1965 Argonne National Laboratory Report No. ANL-7130 (unpublished).

scalar, and pseudoscalar in the interaction Hamiltonian [Eq. (1)] for the decay.

Another reason for making accurate measurements of the helicities of electrons and positrons is to test the *CPT* theorem which asserts that these helicities must be equal and opposite in muon decay.[7] At present, however, the equality of the particle-antiparticle decay rates of π's[8] or μ's[9] is a better test of *CPT* in weak interactions.

We describe here an experiment to measure the helicity of electrons from μ^- decay by Møller scattering. A similar experiment for μ^+ decay has been performed with the same apparatus[10] but will not be discussed here.

II. EXPERIMENTAL METHOD

The Møller scattering method[11,12] was chosen for this experiment, because with the use of spark chambers the analysis of background events is simpler than with the bremsstrahlung transmission method. Moreover, Møller scattering is a single-step process which provides a direct measurement of the polarization, whereas the bremsstrahlung transmission method involves the measurement of the product of two polarizations and is therefore less direct and more difficult to perform accurately.

As compared to earlier helicity measurements,[1,2] the use of spark chambers in this experiment provides a substantial reduction and better understanding of the accidental and background rates, since each event is examined individually.

All the events were processed by computer programs which found the numbers of detected scattering events for opposite magnetizations of the foil and rejected most of the background. These event rates were compared with similar rates obtained from a Monte Carlo program to determine the experimental value of the helicity.

The details of the spin dependence of Møller scattering have been discussed by several authors.[11,13,14] Assuming no transverse polarization of the decay electrons,[15] we require the $e^- - e^-$ scattering cross sections

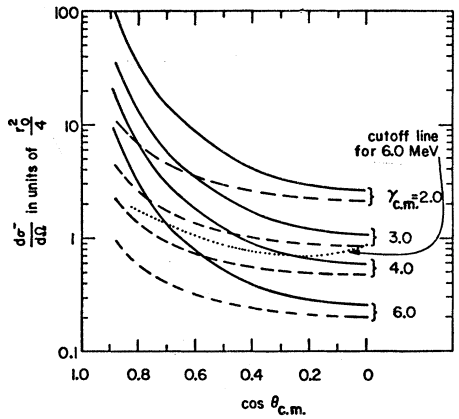

FIG. 1. Møller scattering cross section for polarized electrons. The solid lines give values for the spin-averaged cross section and the dashed lines give corresponding values for the spin-dependent term B in Eq. (3). The dotted line gives the cross section for events with one product having 6.0 MeV total energy.

for incoming electrons with helicity $+1$ and -1. After averaging over the azimuthal angle, the formula for $d\sigma/d\Omega$ in the center-of-mass system reduces to

$$\frac{d\sigma}{d\Omega}=\frac{r_0^2}{2\gamma^2(\gamma^2-1)^2\sin^4\theta}[A\mp B(\hat{p}_1\cdot\hat{\sigma}_2)] \qquad (3)$$

for the helicity of the incident electron equal to ± 1. In Eq. (3), r_0 is the classical electron radius, A and B are quadratic functions of γ^2 and $\sin^2\theta$, where γm_e is the c.m. energy, θ is the polar c.m. scattering angle, $\hat{p}_1$ is a unit vector in the incident direction, and $\hat{\sigma}_2$ is the unit spin vector of the target electron.

Figure 1 shows a graph of the two terms of $d\sigma/d\Omega$ for several values of energy. Our apparatus did not accept events in which one member of the scattered pair had less than 6-MeV total energy. The dotted line labeled "Cutoff", represents the spin averaged cross section [i.e., the first term in Eq. (3)], and indicates the events eliminated by this restriction; only events below this line were accepted.

The polarized target electrons were provided by a Supermendur[16] foil which was magnetized nearly to saturation. The polarization f of the electrons in this foil was found from the relation[12]

$$f=\frac{B}{4\pi n\mu_B}2\left(\frac{g'-1}{g'}\right), \qquad (4)$$

[7] T. Kinoshita and A. Sirlin, Phys. Rev. **108**, 844 (1957).

[8] See, e.g., W. Barkas and A. Rosenfeld, in *Proceedings of the 1960 Rochester Conference on High-Energy Physics* (Interscience Publishers, Inc., New York, 1960), p. 878; R. Durbin, H. Loar, W. Havens, Phys. Rev. **88**, 179 (1952).

[9] See, e.g., S. L. Meyer, E. W. Anderson, E. Bleser, L. M. Lederman, J. L. Rosen, J. Rothberg, and I. T. Wang, Phys. Rev. **132**, 2693 (1963).

[10] S. Parker, C. Rey, and D. M. Schwartz (to be published).

[11] C. Bouchiat and L. Michel, Nucl. Phys. **5**, 416 (1958); L. Grodzins, Progr. Nucl. Phys. **7**, 163 (1959).

[12] J. D. Ullman, H. Frauenfelder, H. J. Lipkin, and A. Rossi, Phys. Rev. **122**, 536 (1961).

[13] A. M. Bincer, Phys. Rev. **107**, 1434 (1957).

[14] G. W. Ford and C. J. Mullin, Phys. Rev. **108**, 477 (1957), **110**, 1485 (1958); see also A. Raczka and R. Raczka, *ibid* **110**, 1469 (1958); Bull. De l'Acad. Polon **6**, 463 (1958).

[15] In the case of the general parity nonconserving weak-interaction Hamiltonian for muon decay there are two terms in the decay amplitude giving rise to transverse components of polarization (see Ref. 7). One of these terms vanishes if time-reversal invariance holds in muon decay. The other term involves the quantity $(p_e\times\hat{\sigma}_e)\cdot(p_e\times\hat{\sigma}_\mu)$ and is proportional to $\frac{3}{4}\alpha(1-x)+\beta$, where $\alpha=|g_s|^2-|g_p'|^2$, $\beta=|g_v|^2+|g_v'|^2-|g_A|^2-|g_A'|^2$, and x is one-half the ratio of electron energy to muon mass. The only effect of the presence of transverse polarization on the present experiment would be to produce a value for the helicity less in magnitude than unity since (a) the polarization of the muon is only about 10%, (b) the data analysis included averaging over the azimuthal scattering angles thus eliminating terms in the cross section which contain transverse polarization dependence.

[16] An alloy composed of 49% Fe, 49% Co, and 2% Va. For a discussion of the magnetic properties of Supermendur, see H. L. B. Gold and D. H. Wenny, Elec. Eng. **76**, 208 (1957). We are grateful to the Arnold Engineering Corporation, Marengo, Illinois who supplied and annealed the foils.

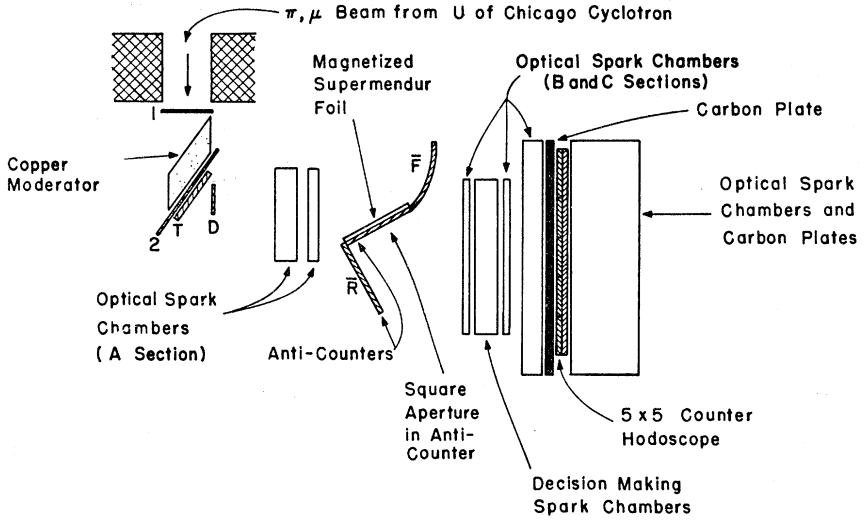

FIG. 2. Diagram of the apparatus showing the positions of the counters, the scattering foil, and the spark chambers. This figure is a plan view; in the elevation view, all the components were placed so as to provide up-down symmetry with respect to a horizontal plane. The scattering foil was magnetized in a horizontal direction.

where B is the magnetic flux density in the foil, n is the electron density, and μ_B is the Bohr magneton. The factor involving the magnetomechanical ratio, $g'[=g/(g-1)$, where g is the gyromagnetic ratio] is the correction for the orbital contribution to the magnetization.[17]

The observed asymmetry, $a_e=(N_2-N_1)/(N_2+N_1)$, where N_i is the number of detected scattering events per incident electron with the foil magnetized in direction i, was about 0.02 in this experiment. The statistical error in this quantity, $\Delta a_e/a_e=1/[a_e(N_2+N_1)^{1/2}]$, is the major contribution to the error in our helicity result. Uncertainties in the low-energy cutoff and in the rate of unpolarized background electrons scattering in the foil were the two most important nonstatistical errors.

III. APPARATUS

The apparatus (Fig. 2) was designed to detect Møller scattering of muon decay electrons in a magnetized foil. The beam, composed of π^-, μ^-, and e^-, was magnetically analyzed and passed through a brass collimator inserted in a 2-ft-thick lead wall, a plastic scintillation counter (1) completely covering the collimator exit, a copper moderator, and a scintillation counter moderator (2) and was stopped in a target (T) composed of $\frac{3}{4}$-in. polyethylene and a scintillation counter. The moderator thickness was adjusted to maximize the number of decay electrons entering the hodoscope through the scattering foil per beam particle (see Fig. 12). Both 2 and T were slanted with their normals at 52° to the beam which permitted the target to be thick in the direction of the beam and yet allow decay electrons to leave it with a minimum of multiple Coulomb scattering, energy loss, and depolarization. A defining counter "D" was placed between the target and the magnetized foil. Counters 1 and 2 were used in anticoincidence to eliminate prompt events and to ensure that the decay electrons originated in the defined target only. Anticoincidence counters R and F surrounded the fiducial area of the foil and a 5×5 counter hodoscope "Hod" was used as a preliminary indicator of a multiple track event. The final determination to pulse the optical spark chambers and photograph an event was made by a set of four decision-making spark chambers (DMSC).[18] These DMSC were used as a low-mass, high-resolution hodoscope to ensure that photographs were taken only for events in which two (or more) tracks appeared in the chambers after the scattering foil. The use of these chambers reduced the background picture-taking rate to about 35% of the total rate as compared with about 95% if only the counter hodoscope was used.

A carbon plate 0.25 in. thick was placed just ahead of the hodoscope (see Fig. 2) to provide a low-energy cutoff for the electrons. This plate in addition to the other material present and the geometrical arrangement gave a cutoff of 6.0±0.5 MeV for electrons produced in Møller scatterings.

A diagram of the electronic logic is given in Fig. 3. To minimize the effects of long-term drifts of counter and spark chamber efficiencies and of beam intensity and spill characteristics, the magnetic field in the foil was reversed automatically at a regular interval. This interval, about 45 sec, was set by a simple neon-tube flasher circuit which drove a bridge of power transistors supplying current to the energizing coils of the foil and two-gate generators for the scalers. A "blocking gate" output was used to gate off the scalers, logic circuits, and spark chamber pulsers during the interval when the magnetic field in the foil was being reversed. The time required to reverse the field was about 110 msec and the length of the blocking gate was set to 420 msec. A

[17] C. Kittel, *Introduction to Solid State Physics* (John Wiley & Sons, Inc., New York, 1956), 2nd ed., pp. 408–414.

[18] C. Rey, S. Parker, B. Sherwood, D. Schwartz, Nucl. Instr. and Methods 32, 217 (1965). We are grateful to V. L. Telegdi who suggested the use of the DMSC for this experiment.

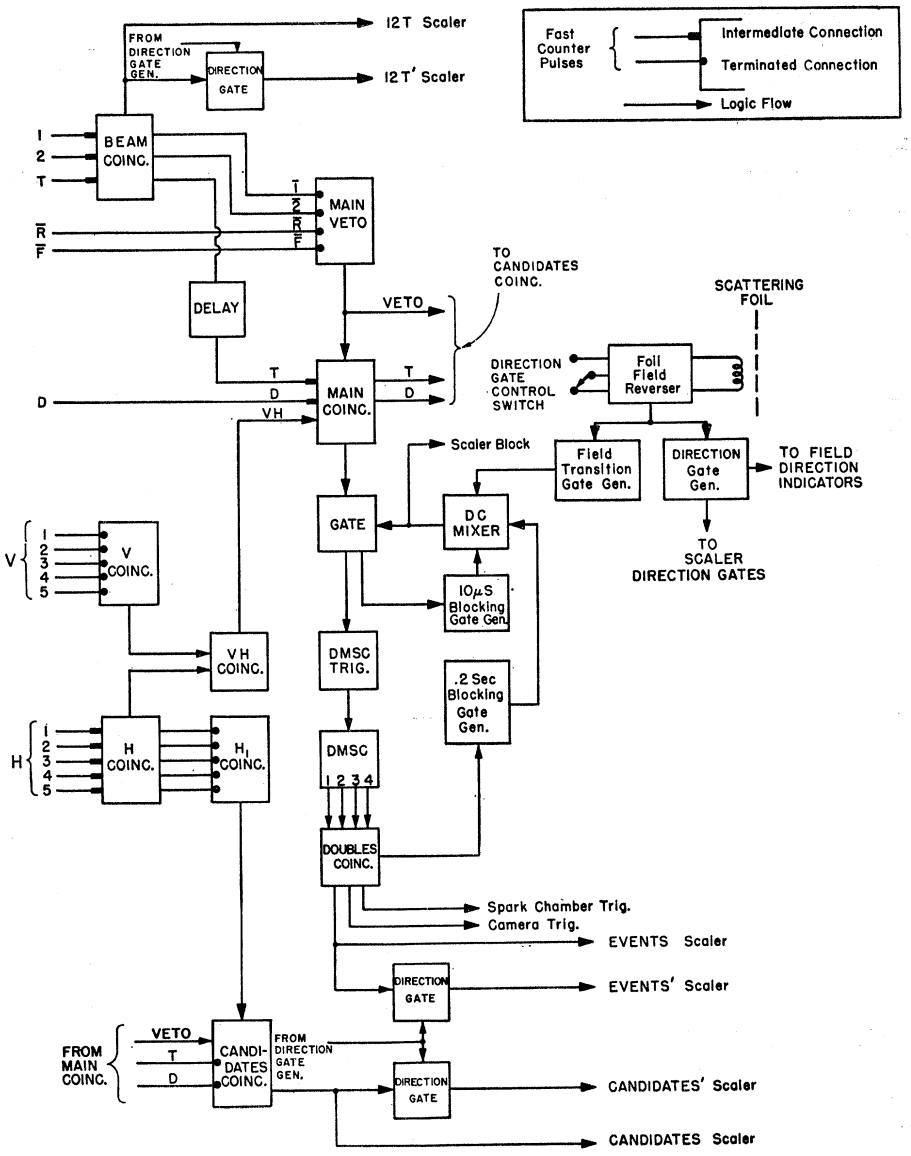

FIG. 3. Block diagram of the electronics logic.

"direction-gate" output was used to gate off three of the scalers (12T', C', and E' in Fig. 3) when the scattering foil was magnetized in one direction in order to provide separate counts for the data taken for each direction of magnetization. The actual field direction for which the primed scalers were gated off was determined by a switch which was reversed for each run of about 1500 pictures. This direction-gate reversing arrangement was introduced to eliminate any bias due to nonuniform performance of the scalers.

Counters 1, 2, and T in coincidence were used as a beam monitor (12T). Another scaler, (12T') controlled by the direction-gate, counted 12T when the foil was magnetized in the specified direction. Counter 1 was scaled independently. The coincidence circuits for the vertical (V) and horizontal (H) sections of the hodoscope were each set for double coincidences (any two of the five) and the "Hod" circuit for singles. Thus a double coincidence in either the V or H sections would give a "Hod" pulse. Pulses from counters 1, 2, R, and F were added, and the sum was used in anticoincidence with T, D, and Hod to form a "Main" coincidence pulse ($M = \bar{1}\bar{2}\bar{R}\bar{F}TD$ Hod) which triggered the DMSC.

A monitor scalar count was obtained from the combination $C = \bar{1}\bar{2}\bar{R}\bar{F}TD\ H_1$. This "candidates" (C) count, as well as a C' count gated by the direction gate, was derived from the use of the H section of the hodoscope connected as a singles counter by the H_1 circuit. The C and C' counts provided a normalization proportional to the rate of decay electrons entering the active region of the apparatus.

The total delay (phototube output pulse to high-

voltage pulse on optical chamber) was 550 nsec of which 220 nsec were used by the DMSC and their associated logic and cables (from the output of the "Main" gate circuit to the output of the DMSC doubles coincidence circuit).

In order to provide range-energy information about those outgoing electrons which did not reach the range chambers, two indicator lights were controlled by the V and H coincidence circuits. When a photograph was taken, one (or both) of these lights would be flashed to indicate which section of the hodoscope contributed to the trigger pulse. Since the electrons had to pass through the V counter in order to reach the H counter, an energy difference of a few MeV was involved.

The scalers and electronic logic were gated off for 10 msec when the DMSC were pulsed. If any two of the four DMSC gave output pulses indicating the presence of more than one track, a double coincidence was formed in the DMSC double coincidence circuit (see Fig. 3) and the optical spark chambers were pulsed. A light-flashing arrangement similar to that used for the hodoscope was employed to indicate which of the four DMSC contributed output pulses. This information was used to measure the efficiencies of the DMSC.

IV. MONTE CARLO CALCULATIONS

Because of the degrading of the electron spectrum in the target, the special geometry, the energy cutoff imposed by the apparatus, and the dependence of the scattering cross section and counting rate asymmetry on these factors, a Monte Carlo prediction of the experimental results was the best method of extracting meaningful information from the data. This Monte Carlo computer program used the known decay spectrum, the scattering cross section given in Eq. (3), the foil electron polarization given by Eq. (4), known formulas for multiple Coulomb scattering, ionization and radiation energy loss, and the specific geometry and logic of the experiment to calculate the counting-rate asymmetry and the absolute event rate and to manufacture scattering events in a format identical to that produced by the data analysis program described below. The two sets of events were processed by a group of programs which displayed the foil and hodoscope illuminations, the multiple scattering distributions and other similar quantities for comparison.

The Monte Carlo program calculated the expected experimental asymmetry by integrating the differential scattering cross section [Eq. (3)] over energy and spin angle with the experimental weighting factors taken into account. This was done as follows. First the solid angle integration was performed analytically with the result

$$I(\gamma,\psi)=\int_{\theta_{\min}}^{\pi/2}\int_{0}^{2\pi}\sin\theta d\theta d\phi\,\frac{d\sigma}{d\Omega}$$

$$=\frac{2\pi r_0^2}{4\gamma^2(\gamma^2-1)^2}\Big[\ln\tan(\theta_{\min}/2)[4\gamma^2-3]$$

$$+\cos\theta_{\min}\Big\{(\gamma^2-1)^2+\frac{2(\gamma^2-1)^2}{\sin^2\theta_{\min}}\Big\}$$

$$+\ln\tan(\theta_{\min}/2)[(4\gamma^2-3)(2\gamma^2-1)]$$

$$-\cos\theta_{\min}[\gamma^4-1]\cos\psi\Big], \quad (5)$$

where

$$\cos\theta_{\min}(\gamma_{\text{c.m.}})=\Big[\frac{\gamma^2_{\text{c.m.}}m_e-E_c}{(\gamma^2_{\text{c.m.}}-1)m_e}\Big], \quad (6)$$

where E_c is the (lab system) cutoff energy for the low-energy outgoing electron, and $\cos\psi=(\hat{\sigma}_1\cdot\hat{\sigma}_2)$.

For each detected event j made by the Monte Carlo program, a contribution P_{ij} to the production probability P_i was calculated. The index i ran from 1 to 2 and indicated the foil magnetization direction. The P_{ij} were given by

$$P_{ij}=nt_jI_{ij}(\gamma_j,\psi_j), \quad (7)$$

where n and t_j and the density of electrons in the foil and the thickness of the foil projected along the incident track, respectively, and I is given by Eq. (5). When a statistically significant number of events J had been accumulated for each magnetization direction, the asymmetry a_n was calculated using

$$a_n=(p_2-p_1)/(p_2+p_1), \quad (8)$$

where

$$p_i=\sum_{j=1}^{J}P_{ij}.$$

This asymmetry was then compared with the experimental value for the processed events to obtain the helicity.

A simplified diagram of the Monte Carlo program appears in Fig. 4. Our assumption of a uniform source distribution in the target was confirmed during the experiment by placing plates of x-ray film before and after the target and observing the uniform exposure over the target area. The electron angular distribution was taken to be isotropic, ignoring the fact that the μ^- were slightly polarized. This was reasonable because of the low degree of polarization ($\sim 10\%$) and because of the relatively small solid angle subtended by the scattering foil. The electron energy spectrum was taken from free

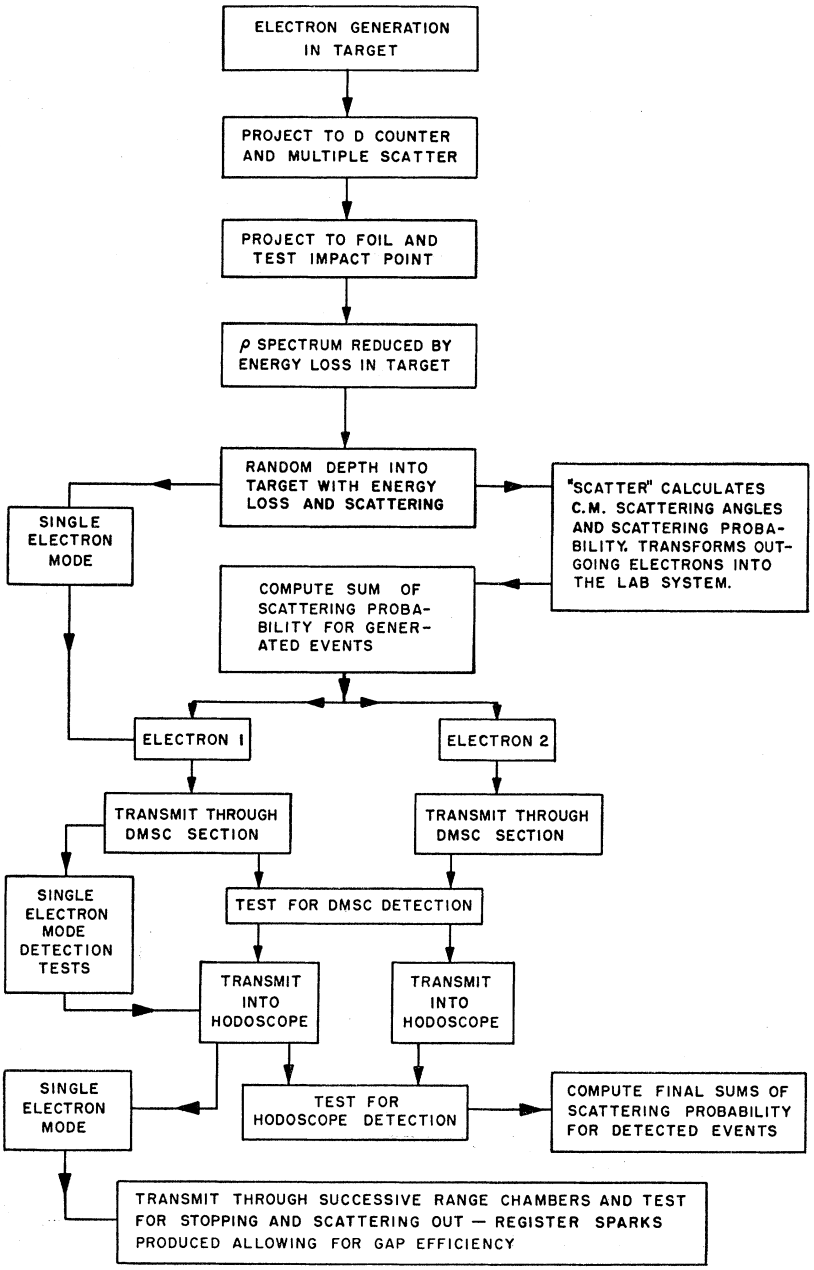

FIG. 4. Simplified flow diagram of the Monte Carlo program.

muon decay[19]

$$dN \propto x^2(3-2x), \tag{9}$$

where x is the ratio of electron energy to $m_\mu/2$.

At every stage of the calculation, energy loss and multiple scattering of the electrons were taken into account. A single Gaussian was used for multiple scattering and the Landau curve[20] was used for ionization loss. The radiation loss was assumed to be exponential with path length.

Those Monte Carlo runs which were used to obtain the asymmetry (as opposed to the energy and angle distributions) calculated the scattering from polarized foil electrons only (i.e., $f=1$). The resulting asymmetry [see Eq. (8)] was then multiplied by f, given by Eq. (4), to obtain the desired comparison with the experimental

[19] It is important to note, with regard to the spectrum, that while the Møller scattering cross section depends strongly on the energy, the asymmetry (or equivalently the ratio $\sigma_{\text{parallel}}/\sigma_{\text{antiparallel}}$) is quite independent of energy above $\gamma \approx 10$ in the lab. This fact is demonstrated by Bincer [Ref. 13, Fig. 1, and Eq. (19)]. This is a fortunate circumstance due to the fact that the bound-state spectrum corrections for μ^- decay in carbon are not well known.

[20] See, e.g., E. L. Goldwasser, F. E. Mills, and A. O. Hanson, Phys. Rev. 88, 1137 (1952).

value. The use of this procedure made the statistical errors in the data and the Monte Carlo asymmetries equal when the ratio of the number of Monte Carlo events to the number of actual events was $f^2 \approx 0.0065$ (see Appendix I).

The efficiencies of the DMSC were used in the calculation since the over-all efficiency depended on the orientation of the plane determined by the two particle tracks relative to the vertical and horizontal planes in which the wires of the DMSC lay.

V. DATA ANALYSIS

All the spark-chamber photographs (about 120 000) were digitized with the CHLOE automatic film scanning system[21] at the Argonne National Laboratory and the data were processed on an ASI-210 computer (part of the CHLOE system) and a CDC-3600 computer.

A general purpose program for the ASI-210, called the LIBERATOR, was used to control the CHLOE scanner and to provide preliminary noise rejection and data consolidation. The details of this program and of the CHLOE system are given elsewhere[21,22] so only a brief description is presented in Appendix III. (See Fig. 5.)

The reproducibility of the CHLOE measurements was more than adequate. Measurements of fiducial separations were maintained to within 0.4% and this error, when combined with the spark measurement errors allowed the coordinates of the centers of the sparks to be determined to within 5 to 8 μ on the film. The demagnification of the optical system in the experiment was 95.4 ± 1.0 so the resulting positions of the sparks in real space were known to about ± 0.7 mm. The resulting radius of confusion about the vertex from this error and from scattering in the B section spark chambers (see Fig. 2) and the DMSC was about 3.0 cm.

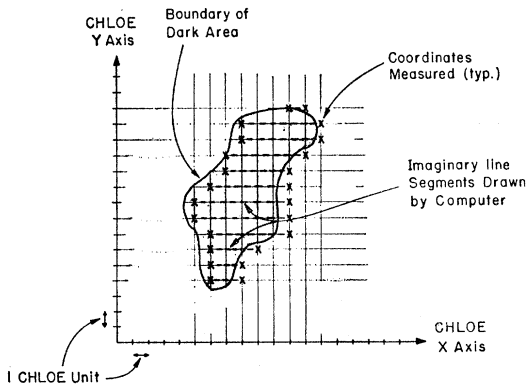

FIG. 5. Response of the CHLOE system to a dark area on the film

[21] D. Hodges, Argonne National Laboratory-Applied Mathematics Division Technical Memorandum No. 61, 1963 (unpublished); R. Clark and W. F. Miller, Methods in Computational Physics (Vol. 5) (Academic Press, New York, 1966), p. 47.

[22] D. Hodges, Argonne National Laboratory Applied Mathematical Division Technical Memorandum No. 100, 1965 (unpublished).

The data produced by the CHLOE system were used as input data for the analysis program CHLOERAMA which was run on the CDC-3600. A simplified flow diagram of this program is given in Fig. 6. The CHLOERAMA program provided most of the event selection and data processing for the experiment.

To process an event, the program first performed tests on the number of sparks appearing in each chamber to determine whether the picture had too many or too few to be a scattering event. Approximately 17% of the pictures were rejected at this point. Next, the spark and fiducial coordinates were transformed into a standard coordinate system. As the transformation was being

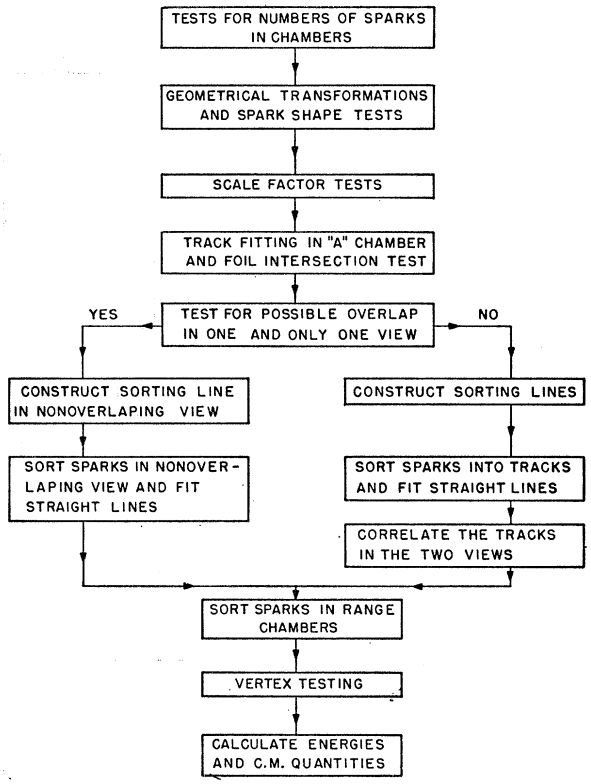

FIG. 6. Simplified flow diagram of the CHLOERAMA data analysis program.

performed, each spark was tested for shape and position relative to the chambers. The scale factors obtained from the fiducial coordinates for the two 90° stereo views were tested independently and required to be within 0.5% of the known (average) values. A least-squares fit to a straight line was then performed on the sparks in the A chamber (see Figs. 2 and 7). The trajectory of the incoming track was required to intercept the fiducial area of the scattering foil. Another 14% of the pictures were rejected here, most of which had more than one track in the A chamber and some of which were the result of inefficiency of the anticoincidence counters surrounding the foil.

The foil impact point determined by the incoming track was used as a pivot for a "sorting" line (see Fig. 7) drawn through it and through a best fit to the average x's (y's) of the sparks in the two B chambers and the C chamber. A special section of the program allowed for a full or partial overlap of the two outgoing tracks in either view since it was possible for the plane of these tracks to be parallel to the optical axis in one view. After sorting the sparks into two tracks for each view an attempt to fit lines was made. Failure to obtain good fits, due either to too many or too few sparks, caused the picture to be rejected. About 25% of the pictures were rejected because of bad fits in the B-C chambers. These rejections were due partly to spark chamber inefficiencies and spurious sparks caused by old tracks. Some rejections here were the result of noise on the film. In some cases noise, extra sparks or tracks, or missing sparks in the A chamber gave an incorrect track fit there and therefore an incorrect foil impact point causing the

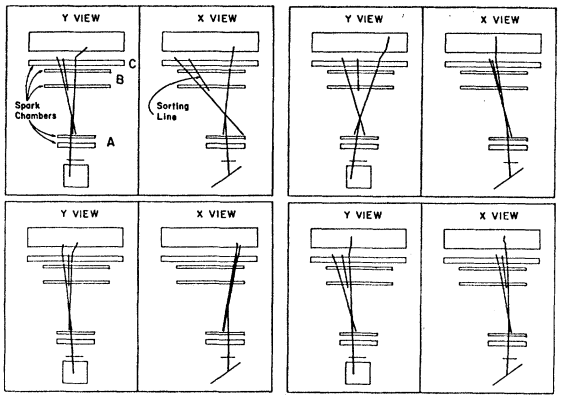

FIG. 7. Computer-produced plot of some typical events.

sorting line to be misplaced. This produced faulty spark sorting and resulted in a bad fit.

The tracks were correlated between the two views by counting the sparks in each track or, if necessary, by forming a correlation number involving the widths (intensities) of the sparks. Hand scanning of about 500 fully processed events revealed only one case of incorrect correlation by the program. Failure to correlate caused the program to reject about 2 to 5 pictures out of each run of 1500.

Four quantities were used for vertex testing. The first two were the distances (R_1 and R_2) of closest approach of the two outgoing tracks to the foil impact point. The second pair involved finding the length L of the shortest line joining the two outgoing tracks and the distance S from its midpoint to the foil point.

From these four quantities, a figure of merit F given by

$$F=(R_1^2+R_2^2+L^2+S^2\tan^2\theta_{\text{opening}})^{1/2}$$

was calculated for each event. In this formula, θ_{opening} is

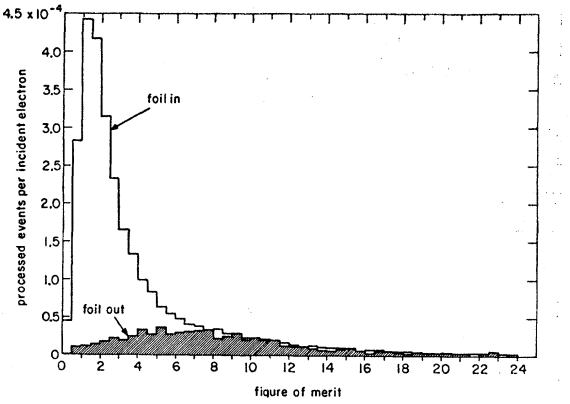

FIG. 8. Figure-of-merit histograms for Supermendur foil data and for no-foil data.

the opening angle between the outgoing tracks. Histograms of F for data taken with Supermendur foil and no foil are shown in Fig. 8. One unit in F corresponds to a radius of confusion about the vertex point of about 0.5 cm. The large size of the vertex region was due to the multiple Coulomb scattering in the B chambers and in the DMSC, which averaged several degrees for the electron energies involved.

The experimental counting-rate asymmetry a_e was plotted against the value of F above which all processed events were rejected. This plot is shown in Fig. 9. It is seen that a_e rises about 20% as the events corresponding

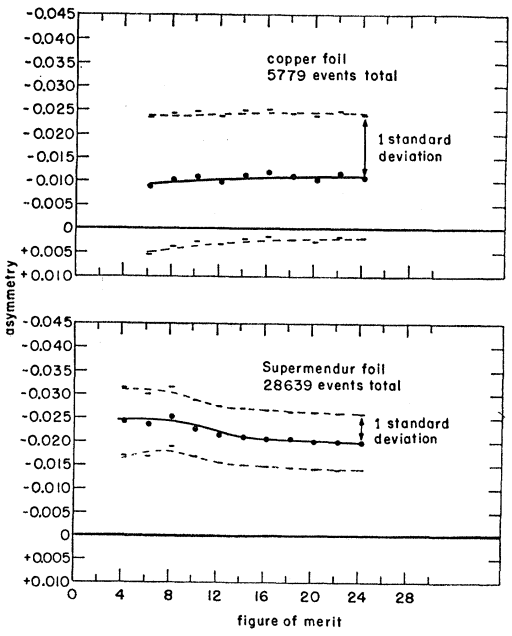

FIG. 9. Plot of asymmetry versus figure-of-merit cutoff for copper foil and Supermendur foil data. The copper-foil plot shows that the asymmetry is consistent with zero and is independent of figure-of-merit cutoff. The Supermendur foil plot shows that the asymmetry is more than three standard deviations away from zero and that it rises by about 20% as the background events with large figures of merit are rejected.

to the no-foil data (see Fig. 8) are rejected. This shows that the foil-independent background (20% of the foil-in event rate) has no measurable asymmetry.

Because of the multiple scattering in the foil and B chamber, it was impossible to obtain meaningful information about the scattering events from the measured lab scattering angles so only the range data were used (see Appendix II). The program followed each track into the range chambers and calculated the range and energy allowing for the unknown penetration depth into the last carbon plate in the track by means of a random number. Thus the uncertainty in energy of the particles was about 15–30%. Nevertheless, the range-energy information was sufficiently good, when averaged over many events, to produce useful center-of-mass scatter plots and histograms (see Fig. 10) which could be compared directly with similar plots for the Monte-Carlo events.

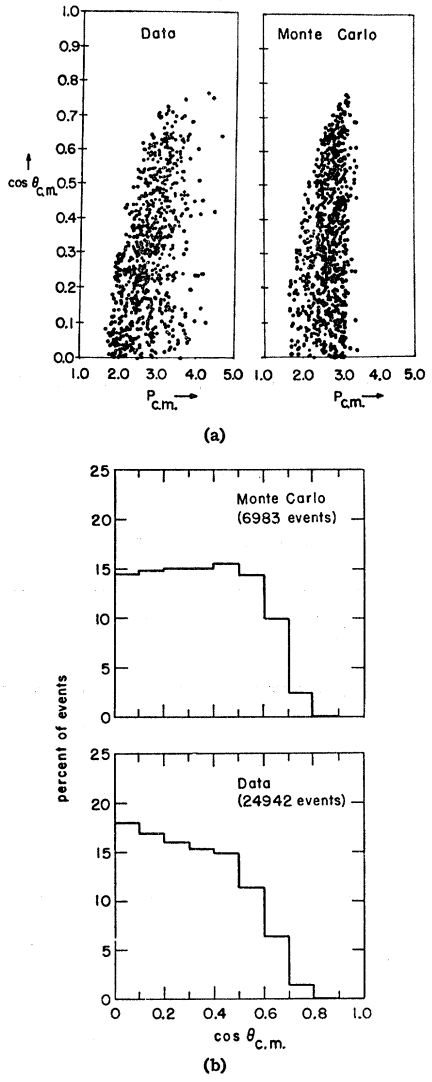

FIG. 10. (a) Scatter plot of c.m. scattering angle versus c.m. momentum for the data and the Monte Carlo events. (b) Histograms of the plots in Fig. 10(a).

It was found that about 40% of the good events were rejected and that these were rejected because of noise on the film, chamber inefficiency, spurious sparks, or missed fiducials. These factors were independent of the magnetization direction in the scattering foil and therefore the measuring could not introduce a significant bias into the asymmetry.

VI. RESULTS

The experimental counting rate asymmetry a_{es}', calculated from unprocessed scaler counts, was found to be

$$a_{es}'=(E_2-E_1)/(E_2+E_1)=-0.0178\pm0.0028,$$

where E_2 (E_1) is the number of pictures taken with the foil magnetized parallel (antiparallel) to the electron beam direction divided by the candidate count accumulated during the interval of parallel (antiparallel) magnetization. The error quoted is the statistical error in the asymmetry based on a total (E_2+E_1) of 80 000 events. Hand scanning showed that approximately 35% of the pictures were background events with no asymmetry, so it may be concluded that the asymmetry for the Møller scattering events $a_{es}=-0.0274\pm0.0045$.

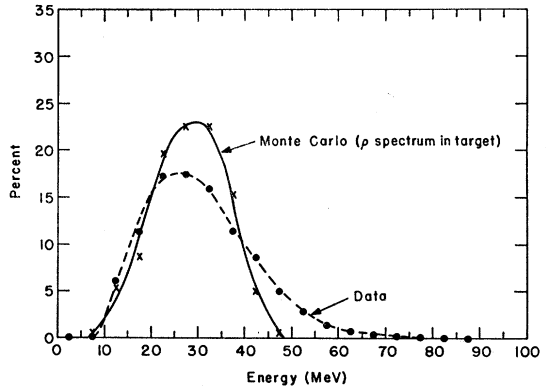

FIG. 11. Spectra of the incident electrons at the scattering point in the foil. These spectra indicate that some of the electrons have an energy higher than the end point of the ρ spectrum.

Figure 9 shows that the asymmetry obtained from the CHLOE processed data depends on the figure of merit cutoff chosen. The variation is caused by the fact that a certain number of background events, having for the most part large figures of merit, have not yet been rejected. Figure 8 shows that the data taken with no scattering foil have a figure of merit distribution with a very broad peak at large figures of merit. This plot is of data which has been processed in the same manner as the data with the foil in place. Thus if we subtract an equal number of events $N(F)$, corresponding to the foil-out event rate at each value of the figure merit F from $N1(F)$ and $N2(F)$ (the number of events with the foil in for the two directions of magnetization), the

TABLE I. Single-electron (candidate) range distribution.

		H counter	Range gaps 1	2	3	4	5	6
Data	Number of events (total=2978)	508	382	405	489	465	382	347
	Percentage	17	13	13	16	16	13	12
Monte Carlo (ρ spectrum)	Number of events (total=5000)	392	668	844	1096	1163	714	123
	Percentage	7.8	13.4	16.9	21.9	23.3	14.3	2.3

asymmetry is essentially independent of the figure of merit cutoff value. The asymmetry obtained in this manner is $a_e'=0.0274\pm0.0068$.

Next we must determine the percentage of the remaining scattering events which are associated with μ^- decay electrons. Figure 11 shows the measured spectrum for the scattering events after degradation by the target, the D counter, and half the scattering foil and the same spectrum as calculated by the Monte-Carlo program using the known muon decay spectrum [Eq. (9)]. Table I gives the results of an analysis of 2978 pictures taken of single electrons (candidates). The numbers and percentages of the candidate electrons reaching each of the range gaps may be compared with similar numbers calculated by a Monte-Carlo program using the muon decay spectrum. The spectral information obtained by both of these methods indicates that $20\%\pm10\%$ of the scattering events were caused by electrons originating from sources other than muon decay. Further evidence for the existence of background electrons is provided by the range curve (Fig. 12) which shows that the electron rate retains about 30% of its maximum value at low values of moderator thickness when the muons pass through the target without stopping. Note that the "Main" coincidence requires a double coincidence in the V or H section of the hodoscope and is therefore unlikely to be satisfied by a scattered primary beam particle.

The most likely process other than μ^- decay involving parity nonconserving interactions which could produce polarized high-energy electrons in this experiment is $\pi^-\rightarrow e^-+\nu$ but the rate for this is at least a factor of 10^4 too small to be comparable with the observed candidate rate of 50/sec. Thus we can conclude that the background electrons are unpolarized. Possible sources of these electrons are discussed in Sec. VII.

Since the scatterings due to the unpolarized electrons have no asymmetry, we correct the experimental asymmetry a_e' for this type of background by dividing by 0.8 ± 0.1. We then obtain the asymmetry $a_e=-0.0342\pm0.0095$, where we have combined the background measurement and statistical errors by taking the square root of the sum of the squares.

The asymmetry for the scattering events predicted by Møller scattering theory assuming equal detection efficiency for both foil polarizations (Fig. 13) is obtained from the formula

$$a_m'=-f\langle\cos\psi\rangle\frac{b(E_c)}{a(E_c)}, \tag{10}$$

where f is the electron polarization in the scattering foil, $\langle\cos\psi\rangle$[23] is the average angle between the spins of the incoming and target particles in the lab,[14] and $b(E_c)$ and $a(E_c)$ are given by

$$a(E_c)+b(E_c)\langle\cos\psi\rangle=\int_{\theta_{\min}(E_c)}^{\pi/2}\sin\theta d\theta \times\int_0^{2\pi}\frac{d\sigma}{d\Omega}(\gamma_{c.m.},\theta_{c.m.},\varphi,\psi), \tag{11}$$

where $\cos\theta_{\min}(\gamma_{c.m.},E_c)$ is given by Eq. (6). Bincer[13] has shown that the asymmetry in the cross sections for parallel and antiparallel spin states is independent of $\gamma_{c.m.}$ for $\gamma_{c.m.}\gtrsim2$ so if we evaluate (11) at, say, $\gamma_{c.m.}=0.5$ as a function of E_c, the result, shown in Fig. 13, will be applicable to the present experiment and will be independent of the electron spectrum. This figure also shows

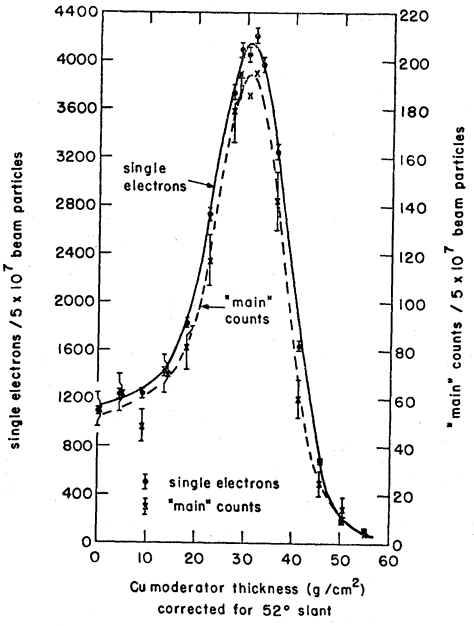

FIG. 12. Range curve showing electron rate versus moderator thickness. The fact that there remains a substantial electron rate at zero moderator thickness shows that there is a source of background electrons.

[23] The uniformity of the direction of the magnetic field in the foil was verified during the experiment by placing a mixture of iron filings and viscous silicone fluid against the magnetized foil and observing that the filings became aligned parallel to the edge of the foil over its entire extent.

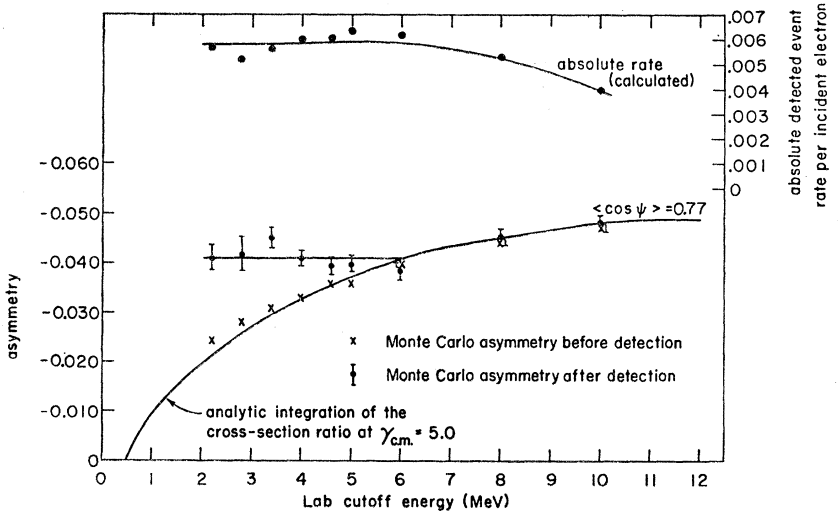

FIG. 13. The variation of absolute detected event rate and predicted event rate asymmetry with laboratory cutoff energy.

the variation of the absolute rate of scattering per incident electron with E_c. The absolute rate is also essentially independent of the spectrum as can be inferred from Fig. 1.

The Monte Carlo program was used to calculate an effective cutoff energy E_c by allowing for the distribution of lab scattering angles, multiple scattering, and range-energy straggling and to determine the detection efficiencies for the scattering events for each direction of foil magnetization. One would expect the asymmetry of the detected events to be only slightly higher than that given by Eq. (10) at a given E_c, since the asymmetry is most pronounced at $\theta_{c.m.}=90°$ which produces outgoing particles of equal energies and at the minimum opening angle in the lab. Figure 13 also shows the Monte Carlo results for asymmetry and absolute rate as a function of E_c. It is seen that for $E_c<6.0$ MeV the Monte Carlo asymmetry remains constant as expected.

The exact value of E_c is subject to some uncertainty because the details of efficiency of the hodoscope scintillation counters versus energy for stopping electrons are not known. The exact amount of energy which must be lost by an electron stopping the first few millimeters of the counter in order for it to count is determined by such factors as scintillator saturation, light-collection efficiency, and photoelectron statistics which are difficult to evaluate precisely in a threshold situation such as this. So we must include systematic errors in the Monte Carlo asymmetry and absolute rate calculations corresponding to an uncertainty in E_c of about ± 0.5 MeV.

The effect of the depolarization of the electrons in the target and in the foil can be estimated from the work of Olsen and Maximon.[24] They show that one can define a "depolarization length" similar and related to the radiation length for a material. For longitudinally polarized electrons, the formula is

$$L_{\text{dep}}=3L_{\text{rad}} \tag{12}$$

for depolarization by bremsstrahlung. The muon decay electrons pass through 0.19 radiation lengths of material (target, D counter, A section spark chambers, and the first half of the scattering foil) which gives a depolarization length of 6.3%. We correct for this effect by multiplying the Monte-Carlo asymmetry by 0.937 before comparing it with the experimental value.

It has been shown[25] that depolarization due to multiple Coulomb scattering is negligible compared to the bremsstrahlung effect discussed above.

With regard to the event rate calculation, the absolute double coincidence efficiency of the hodoscope, which was assumed equal to unity in the calculation, was certainly less than unity in the experiment because of the detection threshold problem discussed above and so the absolute scattering rate calculated by the program should be somewhat higher than that actually measured.

The final results for the asymmetries and absolute rates are given in Table II. From these numbers, we obtain the experimental result that the helicity is $-a_e/a_m=-0.89\pm 0.28$. The ratio of the experimental to the calculated absolute rates is 0.80 ± 0.1.

VII. SYSTEMATIC ERRORS

Contributions from several types of systematic errors are possible in this experiment. Each of the possible sources of systematic error has been considered, and the results are listed below:

A. Errors Built into the Apparatus

(i) Since different scalers were used to count candidates for the magnetization directions, there could have been a difference in the thresholds which would influence the asymmetry. This error was eliminated in two ways.

[24] H. Olsen and L. C. Maximon, Phys. Rev. **114**, 887 (1959).

[25] C. Bouchiat and J. M. Lévy-LeBlond, Nuovo Cimento **33**, 193 (1964); C. K. Iddings, G. L. Shaw, and Y. S. Tsai, Phys. Rev. **135**, B1388 (1964).

TABLE II. Final asymmetries and absolute rates.

	Asymmetry $=(N_2-N_1)/(N_2+N_1)$	Absolute rate (detected events/ incident electron)
Data based on 28 639 processed events)	-0.0342 ± 0.0095	0.0045 ± 0.0005
Monte Carlo (helicity $=-1.0$)	-0.0384 ± 0.0030	0.0054 ± 0.0002

First, the two sets of scalers were set up to count identical groups of pulses and the results were equal to 1 part in 10^4. In addition, the roles of the two sets of scalers were reversed every 1500 events ($\sim$2 h).

(ii) The counting rates of each individual counter were tested and found to be independent of the direction of the foil magnetization to within 1 part in 10^4.

(iii) All known biases of a purely geometrical nature were included and therefore accounted for in the Monte-Carlo program.

(iv) There was a systematic bending of the electrons both in the scattering foil and in its fringing field and this could render the detection efficiency different for the two magnetization directions. This effect was not included in the Monte-Carlo program for two reasons. First, the angles of bending, on the average, were less than one-half of the average multiple Coulomb scattering angles. Second, and more important, the apparatus was symmetric about the horizontal plane in which the magnetic field vector lay thus tending to cancel any small systematic up-down bending effect.

B. Measurement Errors

(i) If the transistor bridge circuit driving the energizing coils for the scattering foil were unbalanced, there might have existed different magnitudes of the field in the two directions. This effect was rendered negligible by using a current-regulated power supply for the circuit. The driving currents were measured to be no more than 5% different for the two directions. Moreover, the foil was so nearly saturated that the resulting difference in its magnetization was less than 0.5%.

(ii) The systematic bias in event rejection during the data processing was negligible. It was found by hand scanning that good events were rejected only for reasons which were independent of the magnetization direction.

(iii) The magnetic field in the scattering foil was measured using a search coil wrapped tightly around the foil and a Tektronix type 555 oscilloscope. When the foil magnetization was reversed, the induced voltage appearing across the coil was displayed as a function of time on the oscilloscope and the waveform was photographed. The vertical and horizontal scales of the oscilloscope were calibrated using standard cells, precision resistors and the 60-cps line frequency. Photographs were made of the calibration traces and a set of scales was made for use in measuring the areas under the magnetization reversal pulses. Several independent measurements were made. It was estimated that the maximum possible systematic error in the measurement of magnetic flux introduced by scale variations, finite trace widths, and measurement errors was 3%.

(iv) The errors in the measurements of the density of the scattering foil were no more than 2%.

C. Other Systematic Errors

(i) The value of the magnetomechanical ratio g' used in Eq. (4), was obtained as a linear interpolation[26] between the values reported[27] for Fe and Co. The value $g'=1.900\pm0.005$ was used, giving a 0.25% contribution to the systematic error.

(ii) The most important systematic errors have already been discussed, namely the uncertainties in the cutoff energy and in the background electron rate. A possible source of high-energy background electrons was investigated. (π^-,γ) reactions[28] in the Cu moderator with conversion of the γ rays in either the moderator, 2, or T could produce background electrons. Permitting a small $\bar{1}$ or $\bar{1}\bar{2}$ inefficiency, the electron rate could have been in the region of 1–10 per second. Thus the previously given estimate (based on the spectra and the range curve in Fig. 12) of $20\%\pm10\%$ (i.e., 10 ± 5 per second) is not unreasonable. This effect contributes the principal systematic error in the experiment, ±0.12 in the helicity result.

Another opportunity for systematic error is the possible presence of a spin-dependent background in the scattering events. Estimates were made of the rates of several processes relative to the Møller scattering rate. The backgrounds investigated were as follows:

(i) Bremsstrahlung in the target or D counter followed by (a) conversion of the γ ray in the foil and the detection in the DMSC hodoscope, of the e^+ or e^- in addition to the original electron. The rate of detection of this type of event was 10^{-5}/initial electron. (b) Compton scattering of the γ ray in the foil with detection of the Compton electron. The rate ratio was 2×10^{-6}/initial electron.

(ii) Bremsstrahlung in the foil with (a) and (b) as above. The rates were (a) 10^{-5}/initial electron (b) 3×10^{-6}/initial electron. Thus it is seen that the spin dependence of these processes could not significantly influence the measured asymmetry since the absolute total rates are so small compared with the measured rate of 4×10^{-3}/incident electron.

VIII. CONCLUSIONS

The data have been analyzed both by using scaler counts and by the detailed processing of 120 000 spark

[26] S. J. Barnett and G. S. Kenney, Phys. Rev. 87, 723 (1952).
[27] G. G. Scott, Rev. Mod. Phys. 34, 102 (1962).
[28] H. Davies, H. Muirhead, and J. N. Woulds, Nucl. Phys. (Neth.) 78, 673 (1966).

chamber photographs. The results for the experimental asymmetry are, in both cases, consistent with the asymmetry calculated by Monte Carlo methods with the assumption of 100% electron polarization. A detailed analysis of the data and of the experimental errors involved produces a measured value of the helicity of the electrons from muon decay of -0.89 ± 0.28. The measured and theoretical absolute event rates agreed within 20%.

ACKNOWLEDGMENTS

The author would like to thank Professor V. L. Telegdi for suggesting this experiment and for his help with the design and preliminary data taking; B. A. Sherwood for his work on design and on the wire spark chambers; S. Derenzo, L. Lavoie, T. Luera, and R. Sumner for their assistance during the preparation and data taking. The author is grateful to C. Rey and to S. Parker, who sponsored the first part of the work, for their assistance and guidance throughout the preparation and data taking and for several helpful discussions concerning the data analysis; and R. Winston for his sponsorship and assistance during the data analysis. The hospitality and assistance given by the Applied Mathematics Division at the Argonne National Laboratory is gratefully acknowledged. The author wishes to thank Professor R. H. Hildebrand for the use of his measuring facilities and for his support of some of the computational work at Argonne.

The author is especially pleased to acknowledge the contribution of D. Hodges whose work made possible the use of the CHLOE system for the data processing and thereby significantly improved the results of the experiment.

APPENDIX I. STATISTICAL ERRORS IN THE ASYMMETRY

We define α to be the counting rate asymmetry in the case that all the electrons in the scattering foil are polarized ($f=1$). In general the observed asymmetry a is given by $a=f\alpha$.

If N_e and N_{MC} are the total numbers of scattering events in the experiment and in the Monte-Carlo computations, respectively, the corresponding relative statistical errors in the asymmetries are given by

$$\epsilon_e=\frac{\Delta a}{a}=\frac{1}{a(N_e)^{1/2}},$$

$$\epsilon_{\mathrm{MC}}=\frac{\Delta\alpha}{\alpha}=\frac{1}{\alpha(N_{\mathrm{MC}})^{1/2}}.$$

If these two relative errors are to be equal, we must have

$$\frac{1}{a(N_e)^{1/2}}=\frac{1}{\alpha(N_{\mathrm{MC}})^{1/2}}$$

or

$$N_{\mathrm{MC}}=f^2N_e.$$

APPENDIX II. ERRORS IN CENTER-OF-MASS VARIABLES FOR INDIVIDUAL EVENTS

We are interested in the center-of-mass momentum (of each electron) $P_{\mathrm{c.m.}}$ and the cosine of the center-of-mass scattering angle, $\cos\theta_{\mathrm{c.m.}}$. In the present experiment, it is possible to measure four relevant quantities for each event: the lay system energies of the two outgoing electrons, E_1 and E_2, and the lab system scattering angles θ_1 and θ_2. The question of which lab quantities to use is answered by a simple error analysis as follows.

The c.m. momentum as computed from the lab energies and lab angles, respectively, is given by

$$P_{\mathrm{c.m.}-E}=[\tfrac{1}{2}m_e(E_1+E_2-2m_e)]^{1/2}, \quad \text{(A1)}$$

$$P_{\mathrm{c.m.}-A}=m_e(\cot\theta_1\cot\theta_2-1)^{1/2}, \quad \text{(A2)}$$

where m_e is the electron rest mass. The relative errors in these quantities are given by

$$\frac{\Delta P_{\mathrm{c.m.}-E}}{P_{\mathrm{c.m.}-E}}=\frac{1}{P_{\mathrm{c.m.}-E}}\times\left[\left(\frac{\partial P_{\mathrm{c.m.}-E}}{\partial E_1}\Delta E_1\right)^2+\left(\frac{\partial P_{\mathrm{c.m.}-E}}{\partial E_2}\Delta E_2\right)^2\right]^{1/2}$$

$$=\frac{m_e}{4P_{\mathrm{c.m.}-E}}[\Delta E_1{}^2+\Delta E_2{}^2]^{1/2}, \quad \text{(A3)}$$

and similarily

$$\frac{\Delta P_{\mathrm{c.m.}-A}}{P_{\mathrm{c.m.}-A}}=\frac{m_e{}^2}{2\sin\theta_1\sin\theta_2 P_{\mathrm{c.m.}-A}{}^2}\times\left(\frac{\cos^2\theta_2}{\sin^2\theta_1}\Delta\theta_1{}^2+\frac{\cos^2\theta_1}{\sin^2\theta_2}\Delta\theta_2{}^2\right)^{1/2}. \quad \text{(A4)}$$

Let us consider a typical scattering event. Let $E_1=20$ MeV, $E_2=10$ MeV, or, $\theta_1=0.2425$, $\theta_2=0.3415$. We obtain, using (A1) or (A2), $P_{\mathrm{c.m.}}=2.64$ MeV/c. The width of the Landau straggling curve for energy loss is approximately 20% of the energy loss. Furthermore, there exists an uncertainty in the stopping point of the average scattered electron in this experiment of about ±2 MeV. So a reasonable random energy error is given by $\Delta E=0.3\ E$, or 30% error. One-half the scattering foil contains about 0.08 radiation length which gives $\Delta\theta\simeq0.2$ rad and $\Delta\theta\simeq0.4$ rad for the rms multiple Coulomb scattering angles. Substituting these values into (A3) and (A4), we obtain

$$\Delta P_{\mathrm{c.m.}-E}/P_{\mathrm{c.m.}-E}=0.12,$$

and

$$\Delta P_{\mathrm{c.m.}-A}/P_{\mathrm{c.m.}-A}=0.30.$$

For the c.m. scattering angle cosine, we have

$$\cos\theta_{\text{c.m.}-E}=\frac{|E_1-E_2|}{E_1+E_2-2m_e}, \tag{A5}$$

$$\cos\theta_{\text{c.m.}-A}=\frac{|\cot\theta_1-\cot\theta_2|}{\cot\theta_1+\cot\theta_2}, \tag{A6}$$

and

$$\frac{\Delta\cos\theta_{\text{c.m.}-E}}{\cos\theta_{\text{c.m.}-E}}=\frac{2}{|E_1-E_2|(E_1+E_2-2m_e)}\times[(E_2-1)^2\Delta E_1^2+(E_1-1)^2\Delta E_2^2]^{1/2}, \tag{A7}$$

$$\frac{\Delta\cos\theta_{\text{c.m.}-A}}{\cos\theta_{\text{c.m.}-A}}=\frac{2}{\sin\theta_1\sin\theta_2|\cot\theta_1^2-\cot\theta_2^2|}\times\left(\frac{\cos^2\theta_2}{\sin^2\theta_1}\Delta\theta_1^2+\frac{\cos^2\theta_1}{\sin^2\theta_2}\Delta\theta_2^2\right)^{1/2}, \tag{A8}$$

which gives $\cos\theta_{\text{c.m.}-E}=0.357$ and

$$\frac{\Delta\cos\theta_{\text{c.m.}-E}}{\cos\theta_{\text{c.m.}-E}}=0.56,$$

$$\frac{\Delta\cos\theta_{\text{c.m.}-A}}{\cos\theta_{\text{c.m.}-A}}=12.30.$$

Thus it is clear that the use of the lab energies is the best method of calculating the c.m. quantities in this experiment.

APPENDIX III. DESCRIPTION OF THE CHLOE SYSTEM

The CHLOE system is a programmed flying spot film digitizer. The spot provided by a cathode ray tube (CRT) is stepped across specified areas of the film and the light transmitted through the film is viewed by a photomultiplier tube. The coordinates of the spot are sent to the ASI computer whenever a black-white boundary is encountered. The intensity of the spot of light produced by the CRT can be set to any one of 1024 values. Thus if there is a dark area on the film (a spark image) the scanner will produce the coordinates of the two edges of the area on each pass. A line segment (imaginary) is drawn between each pair of points so determined (see Fig. 5) and the LIBERATOR program correlates these segments by requiring a minimum number of segments each of a minimum length and each having a minimum overlap with its neighbor for a given spark image.

When the requirements have been satisfied, the LIBERATOR performs a series of calculations. For example, in the case of sparks, the average x and y coordinates (see Fig. 5) for the dark area, the first x and y and the last x and y coordinates, and the area (i.e., the sum of the lengths of all the line segments) are computed and these numbers are written on the output magnetic tape. In the case of an indicator light, only the number of line segments obtained is written out. By setting these requirements to values appropriate for the sizes and shapes of sparks, a satisfactory level of noise rejection was attained.

The LIBERATOR program was set up for almost fully automatic operation of the measuring machine. Since the film was not prescanned, every picture was digitized. Under normal conditions, operator intervention was required only when the machine missed the initial reference fiducial or encountered a blank frame. These failures occurred for less than 0.5% of the pictures.

The measuring sequence began with the machine searching a preset area on the frame for the first reference fiducial. When this fiducial was found, a preliminary sweep of part of the frame was made at low point density and the number of line segments was counted. If this number was within specified limits, the sequence continued; otherwise the intensity of the CRT light was adjusted appropriately and another sweep of the frame made. This procedure corrected for long-term drifts in the discriminator and phototube circuits. The next step was to normalize all the scanning areas to the coordinates of the reference fiducials. Then 12 spark chamber areas, five fiducial areas, and nine indicator light areas were measured as described above. The scanning conditions were adjusted for best signal-to-noise ratio in each area. Approximately 350 pictures per hour were measured in this manner.